L-CHANGING COLLISIONS IN COLD RYDBERG GASES

A. WALZ-FLANNIGAN, D. FELDBAUM, S. K. DUTTA, J. R. GUEST, G. RAITHEL
Department of Physics, University of Michigan, Ann Arbor, MI 48109-1120, USA
E-mail: graithel@umich.edu

Using spectroscopic methods and time-resolved electron counting, it is found that clouds of cold Rydberg atoms can emit electrons over a surprisingly long time scale. Our observations are explained by l-mixing collisions between Rydberg atoms and slow electrons. The thereby created high-angular-momentum Rydberg atoms thermally ionize slowly and with large probabilities. Calculations supporting this explanation are presented.

1 Introduction

Laser-cooled atoms can be excited into Rydberg states to study the behavior of Rydberg atoms at both high densities and low atomic velocities. Cold Rydberg atom gases have been found to undergo virtually complete ionization if the density of the excited Rydberg atom population exceeds a critical value dependent on the principal quantum number [1]. Ionization avalanches triggered by ionizing collisions between Rydberg atoms appear to play a role. Ionization avalanches have also been observed in hot Rydberg gases [2]. At conditions such that ionization is not dominant, processes with rate constants even larger than those of ionizing processes can be observed. Non-ionizing interactions of Rydberg atoms include l-mixing collisions, which are the main subject of this report, and resonant electric-dipole interactions [3,4]. Resonant electric-dipole interactions as well as interactions between Rydberg states with permanent electric-dipole moments are promising candidates for the implementation of quantum-logic operations [5]. In dense clouds of Rydberg atoms one might also find a novel class of Rydberg molecules, which has recently been predicted [6]. Other recent work in the field includes the observation of efficient recombination of expanding cold plasmas into Rydberg atoms [7].

Here, we report the spontaneous evolution of cold Rydberg atoms into long-lived states. These states reveal themselves via a long-lasting electron emission signal, the time scale of which exceeds the natural lifetime of the initially excited Rydberg levels by at least two orders of magnitude. We identify the long-lived states as high-l Rydberg states, and explain their appearance by l-changing collisions between slow, free electrons and the initially excited low-l Rydberg atoms. A similar process is at work in molecular ZEro Kinetic Energy (ZEKE) spectroscopy [8].

2 Experimental Setup

In our experiment, a vapor cell (pressure $< 5 \times 10^{-9}$ Torr) magneto-optic trap (MOT) is operated in a 10 Hz cycle. ^{87}Rb atoms are cooled to ~ 50 μK and trapped for 75 ms, after which the MOT light and magnetic fields are turned off. Subsequently, the atoms are cooled further by an optical molasses for about 1 ms. Then, a 5 μs long diode laser pulse ($\lambda = 780$ nm) resonant with the $5S_{1/2}, F = 2 \rightarrow 5P_{3/2}, F = 3$ transition is applied, exciting a fraction of the ground state atoms to the $5P_{3/2}$ level. While the 780 nm pulse is on, a tunable blue dye laser pulse ($\lambda \approx 480$ nm, pulse width ≈ 10 ns, bandwidth ≈ 15 GHz, pulse

energy < 5 mJ) illuminates the entire atom cloud and excites $5P_{3/2}$ atoms to s- and/or d-Rydberg states. The dye laser is pumped by a tripled Nd:YAG laser and consists of an oscillator and two optional stages of amplification. A microchannel-plate (MCP) detector placed 10 cm from the atom cloud is used to detect electrons emitted from the Rydberg gas. No electric field ionization pulse is applied. Based on the Rydberg excitation spectra obtained in this experiment, the electric field due to the MCP at the location of the atoms is estimated to be $<$ 0.5 V/cm. Due to the weakness of the electric field at the location of the atom cloud, field ionization of Rydberg states with principal quantum numbers lower than about 100 does not contribute to the electron current emanating from the Rydberg gas. However, the Rydberg atom gas emits electrons due to other processes, which are studied in this report. The released electrons are collected by the weak MCP electric field. In the immediate vicinity of the MCP, the electric field increases and accelerates the electrons to 50eV. A photon counter records the MCP pulses over a window with variable delay and width. We measure the dependence of the electron signal on time, the wavelength of the blue laser, and the Rydberg atom density.

As another diagnostic tool, we use a weak probe laser pulse that has a duration of a few μs and is resonant with the $5S_{1/2}, F = 2 \rightarrow 5P_{3/2}, F = 3$ transition. The probe laser has an intensity much smaller than the saturation intensity of that transition (1.6 mW/cm^2) and a diameter smaller than that of the atom cloud. The probe laser pulse is used to measure the central area density of ground-state atoms contained in the atom cloud.

3 Experimental Results

3.1 Time Dependence of the Electron Emission

Among the evidence for $l-$mixing we have gathered, the most convincing is the appearance of a long-lasting electron emission, which occurs when we excite a bound Rydberg level if the density of Rydberg atoms and the principal quantum number are not too high. Under such conditions, electrons are emitted over an interval of up to 50 ms duration. The time dependence of this long-lasting electron signal is shown in Fig. 1. There, the dye laser was operated at a low pulse energy ($<$ 1 mJ) and at fixed wavelengths. The similarity of the two depicted results is coincidental. The absolute strength of the signal has been found to depend on the quantum numbers of the excited Rydberg state (see Fig. 3) and the laser pulse energies. Further, the signal is sensitive to weak background magnetic fields, indicating that it is due to very slow electrons emanating from the Rydberg gas.

The long-lasting signal is only present if the wavelength of the blue laser is longer than the ionization wavelength ($\lambda_{\rm ion} = 479.1$ nm) and if a bound Rydberg state is excited. To show this, in Fig. 2 we compare the electron signal observed during the first 45 μs for the cases of $\lambda > \lambda_{\rm ion}$ and $\lambda < \lambda_{\rm ion}$. During the first 30 μs, in both cases a large electron current is observed. This electron current reflects the decay of a metastable ultracold plasma, identical to the one observed in Ref. [9]. The plasma plays an important role in the formation of high-l Rydberg states, as discussed in Sec. 4.4. In the case $\lambda < \lambda_{\rm ion}$, the electron current entirely ceases after the plasma decay signal. In contrast, if the initial excitation produces a gas of bound Rydberg atoms, a long-lasting electron signal with a large integrated charge appears after the plasma has decayed.

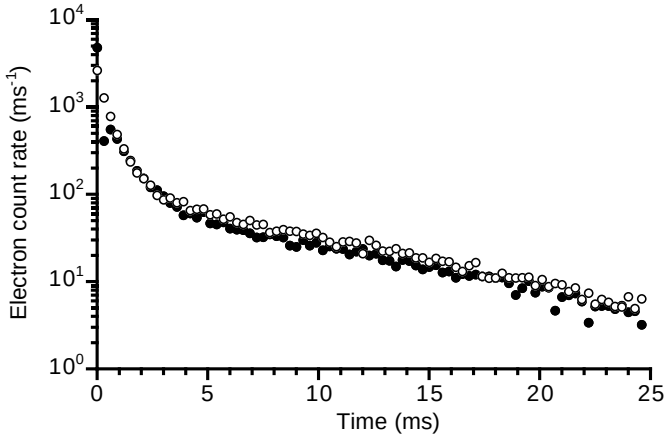

Figure 1. Electron signal vs. delay time from the Rydberg atom excitation, observed for the excitation of 20*d*- (open circles) and 50*d*-states (full circles). The initial number of Rydberg atoms is 10^6 and 10^5, respectively. The difference in the Rydberg atom numbers is due to the different degrees of saturation of the transitions populating the Rydberg states. The cloud volume is $\sim$1 mm^3.

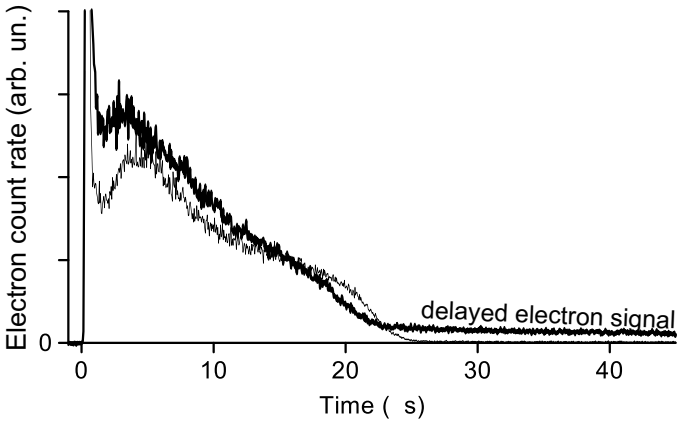

Figure 2. Short-time behavior of electron emission during the first 45 μs for excitation above the photoionization threshold ($\lambda < 479.1$ nm, thin curve) and below ($\lambda = 483$ nm, thick curve). Only in the case that bound Rydberg atoms are excited does the electron signal exhibit a long-lasting tail, the beginning of which is indicated in the figure.

3.2 Spectral Dependence of the Delayed Electron Signal

By fixing the delay of the photon counter gate at a value larger than the plasma decay time and scanning the dye laser, we measure how the long-lasting electron signal depends on the wavelength of the blue laser. The resultant spectra, an example of which is shown in Fig. 3, show that the delayed electron signal is present only when the dye laser is tuned to a bound Rydberg resonance, and that the signal does not appear when the dye laser is

tuned between bound Rydberg resonances or above the ionization limit ($\lambda_{\rm ion} = 479.1$ nm).

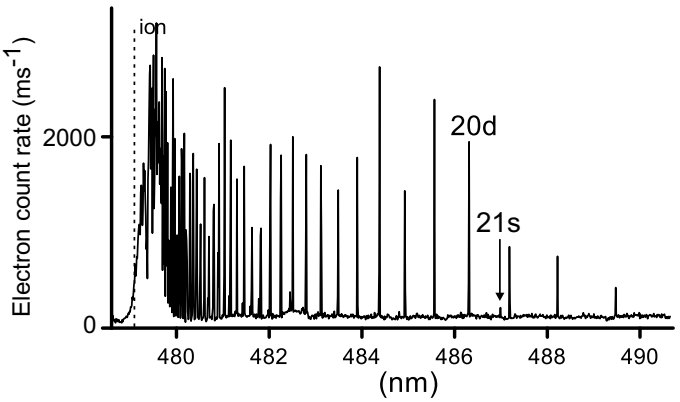

Figure 3. Delayed electron signal vs. excitation wavelength, measured 10 ms after the Rydberg excitation pulse.

We have observed the delayed electron signal for Rydberg atom numbers as small as a few 10^3. Under such conditions, the delayed electron signal ranges from principal quantum numbers $n \sim 50$ up to the ionization limit, the lower limit being very sensitive to the detailed conditions (atom number in the MOT, laser pulse energies etc.). The data in Figs. 1-3 are obtained for moderate Rydberg atom numbers (10^5 at high n to 10^6 at low n) and principal quantum numbers that are not too high. When the number of Rydberg atoms is increased further, the range over which the long-lasting electron signal occurs is observed to shift to lower n. With both the $5S_{1/2}, F = 2 \rightarrow 5P_{3/2}, F = 3$ transition and the Rydberg transition near saturation, we excite a few 10^6 Rydberg atoms, independent of n. Under such conditions, the long-lasting electron signal occurs over an approximate range of $35 > n > 12$.

3.3 Trap Loss Measurements

Using the probe laser mentioned in Sec. 2, we have measured the area density of atoms in the trap vs. the wavelength of the blue laser under conditions where both the $5S_{1/2}, F = 2 \rightarrow 5P_{3/2}, F = 3$ transition and the Rydberg transition have been near saturation. Varying the time at which the probe pulse measures the trap density, we have first found that the observed trap loss is permanent, i.e. it reflects the loss of atoms due to an ionizing process which does not allow the affected atoms to return into the trapping cycle of the MOT. The damage which the Rydberg atom excitation does to the atom trap population is measured by the loss in area density inflicted by a single Rydberg excitation cycle divided by the area density immediately before that Rydberg atom excitation. In the following, we denote this single-shot loss ratio by X. In quasi-steady-state, atoms get continuously collected by the atom trap with a certain loading rate. The loading is balanced by the inherent losses of the atom trap, which are mostly due to background gas collisions, and the losses inflicted by the Rydberg atom excitation that happen at a repetition rate of 10 s^{-1}. We have used the

equilibrium between atom losses and gains to calculate the single-shot loss ratio X from area density measurements.

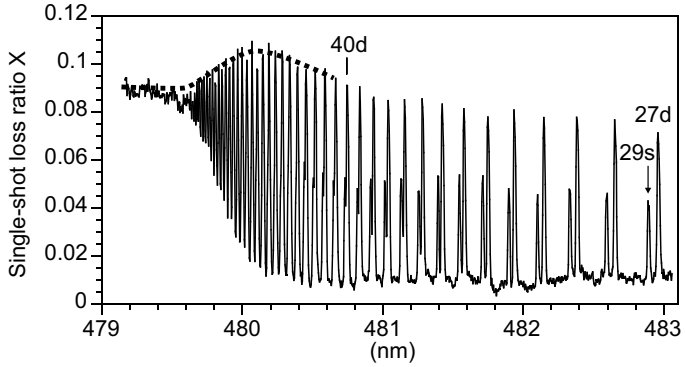

Figure 4. Single-shot loss ratio X vs. wavelength of the blue laser, when both the $5S_{1/2}, F = 2 \rightarrow 5P_{3/2}, F = 3$ transition and the Rydberg transition are near saturation.

In Fig. 4 we show how X depends on the wavelength of the blue laser. Near the ionization threshold and above, direct photoionization removes $\approx 9\%$ of the trapped atoms per shot. Below the threshold, individual Rydberg excitation lines become resolved for n less than about 80. The peaks in X occur down to $n = 17$ (peaks $17d$ to $26d$ not shown in Fig. 4). In contrast, the delayed electron signal observed for conditions such as in Fig. 4 displays peaks only over a range $35 > n > 12$ (shown in Ref. [10]). Thus, in an approximate range of $80 > n > 35$ the trap loss spectrum exhibits clear peaks that do not have corresponding peaks in the delayed electron signal. Further, in the range $80 > n > 35$ the height of the peaks observed in X displays a broad maximum, highlighted by a thick dashed line in Fig. 4. We have consistently observed this maximum and are certain that it is real.

4 Explanation of the Experimental Results

4.1 Summary of our Interpretation

The source of the detected delayed electrons and the reasons for the long time scales associated with their emission are a main subject of this report. The key element in our explanation is that Rydberg atoms are transferred from their initial low angular momentum states ($l = 0$ or 2) into an approximately statistical mixture of lm-states. The natural lifetime of low-l states scales as n^3, while for a statistical mixture of lm states it scales as $n^{4.5}$ (see Ref. [11]). From the considerations developed in the following sections we conclude that the transfer of population into high-l states originates from l-mixing due to collisions of Rydberg atoms with by-passing "early" electrons. The l-mixing phase lasts of order 50 μs. Subsequently, the long-lived high-l-atoms in the mixture of Rydberg atoms decay over tens of milliseconds. The decay occurs in large part by thermal ionization in the ambient 300K black-body radiation. The thereby released thermal electrons are detected as the "delayed" electrons, shown in Figs. 1-3.

4.2 General Considerations about l-mixing

It is known that l-mixing collisions between Rydberg atoms and charged particles have immensely large cross sections. Many experiments ([12] and references in [11]) and theoretical studies [8,13] have been carried out to understand these collisions. The l-mixing cross sections are particularly large if the collision velocity is of order or smaller than the classical Kepler velocity of the involved Rydberg atoms. The l-mixing collision rate of a slow Rydberg atom embedded in a cloud of charged particles with density n_e and velocity v is $R = n_e\sigma(v)v$. The rate R is expected to have a maximum in the vicinity of the Kepler velocity. For velocities much larger than the Kepler velocity, the rate R drops due to a rapid decline of the cross section $\sigma(v)$ with v, while for much lower velocities, where $\sigma(v)$ tends to become constant, R drops due to its proportionality to v.

l-mixing plays an important role in the explanation of the "ZEKE"-effect in molecular spectroscopy [8]. In these experiments, molecules in high-lying Rydberg states are placed in an environment that contains a large density of ions moving at velocities of order of the Kepler velocity of high-lying Rydberg levels (typically $n > 100$). Free electrons in these systems move much faster. As a result, l-mixing in the molecular "ZEKE"-effect is thought to be mostly due to collisions between ions and Rydberg atoms.

In the environment of interest in the present context, ions that may be created are just about as slow as the atoms they are created from, i.e. only of order 0.1 m/s. As a result, in our system l-mixing due to collisions between ions and Rydberg atoms will be ineffective. As discussed in Sec. 4.3, the velocity of free electrons in our system is of order 50000 m/s, i.e. of order of the Kepler velocity of Rydberg states with $n \sim 40$. Thus, in our experiment l-mixing due to collisions between free electrons and Rydberg atoms will be effective.

To claim that l-mixing is important, we show that under situations in which the delayed electron signal occurs the l-mixing probability saturates, i.e. the inequality

$$P = Rt_{\rm int} = n_e\sigma v t_{\rm int} \geq 1 \tag{1}$$

holds. There, $t_{\rm int}$ is the time that is potentially available for l-mixing collisions.

4.3 Sources of "Initial Electrons"

For efficient l-mixing to occur, a reasonably dense cloud of "initial" electrons interpenetrating the Rydberg atom cloud has to be present for a sufficient amount of time, such as to satisfy Eq. (1). Under our conditions (not too high principal quantum numbers and moderate densities), the primary source of early electrons is thermal ionization of the initial Rydberg atom population. To estimate the electron yield due to this process, we have performed rate equation calculations that simulate the radiation-induced transport of the Rydberg atom population. Since we can consider our system to be isotropic, the magnetic quantum number m is of no importance, and transitions between manifolds of levels identified by only n and l occur at rates governed by shell-averaged oscillator strengths [11]. In our simulations, we use a set of bound manifolds $\{(n,l)\,|\,5 \leq n \leq 100, 0 \leq l < n\}$ and a discrete set of free manifolds $\{(\epsilon,l)\,|\,\epsilon = k \times 1.3 \text{ meV }, 0 \leq k \leq 100, 0 \leq l \leq 100\}$, where ϵ denotes the free-electron energy. Continuum lowering caused by the presence of small stray electric fields justifies the restriction of the bound basis to levels with $n \leq 100$. The largest energy of free states included in the calculation is set to be $5k_BT$, where T is the temperature

of the ambient radiation, $T = 300$ K. For any initial level (n_0, l_0), the simulations yield ionization probabilities and energy probability distributions for the thermal electrons.

The time over which electrons can be effective in causing l-mixing is limited. This fact will be validated retro-actively, after the importance of an electron trapping mechanism has been established (Sec. 4.4). For now, we claim that the time interval within which a thermal electron must be released in order to be effective in causing l-mixing is 50 μs. The number of useful thermal electrons equals the initial number of Rydberg atoms times the thermal ionization probability of the initial Rydberg state at 50 μs (not the ionization probability at $t \to \infty$). In Fig. 5 it is shown that the photoionization probability at 50 μs, $\eta_{50\mu s}$, peaks at about 1.8% near $n_0 = 40$. At much lower quantum numbers, $\eta_{50\mu s}$ becomes small because the energy that is required to ionize the atom, $1/(2n^2)$ at.un., is much larger than $k_B T$. As a result, for $n_0 \ll 40$ the atoms preferentially decay back into the ground state rather than getting thermally excited into higher states. For initial quantum numbers $n_0 \gg 40$, $\eta_{50\mu s}$ becomes small because the photoionization *rate* tends to decrease as $\propto n_0^{-3}$ (while the photoionization probability at $t \to \infty$ still increases). Thus, for $n_0 \gg 40$ most thermal electrons are created too late to be effective. Multiplying the values $\eta_{50\mu s}$ given in Fig. 5 with the estimated initial number of Rydberg atoms, we estimate that under the conditions of Fig. 1 the $20d$ and $50d$ states yield of order 5000 thermal electrons.

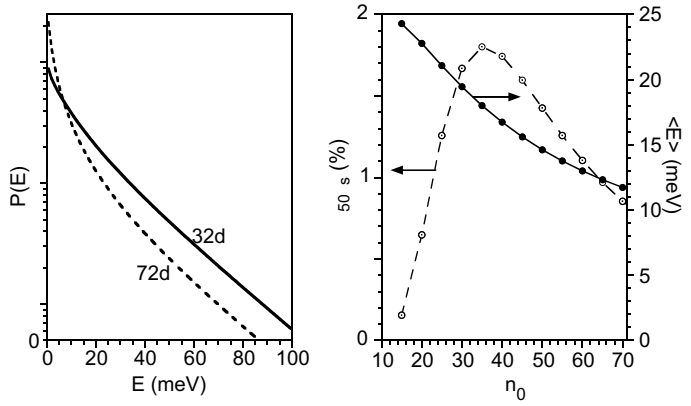

Figure 5. Left: Energy distribution of thermal electrons emitted from the indicated states in a 300K radiation field during the first 50 μs of exposure. Note the logarithmic scale of $P(E)$. Right: Thermal ionization probability $\eta_{50\mu s}$ of nd rubidium atoms placed in a 300K radiation field for 50 μs vs. the principal quantum number n.

The energy distribution of the thermal electrons is highly non-thermal, as it peaks at zero energy. This is shown in the left panel of Fig. 5. Further, the calculations show that the average kinetic energy of the thermal electrons gradually decreases with increasing n_0 (see right panel of Fig. 5). $\langle E \rangle$ is always less than $k_B T = 26$ meV. We have estimated that under the conditions of Fig. 1 other sources of early electrons, including ionizing collisions between cold and hot Rydberg atoms [1], are less important. We have - in summary of this subsection - found that under typical conditions under which a long-lasting electron signal is observed there are a few thousand electrons with energies of order 10 meV available to

engage in collisions with Rydberg atoms.

4.4 Electron Trap

The thermal electrons escape the atom cloud until the cloud is sufficiently positively charged to prevent further electrons from leaving. Note that only few electrons need to leave in order to trap some of the abundant very slow thermal electrons (low-energy peaks in the left panel of Fig. 5). An electron trapping mechanism associated with the excitation of cold atoms into high-lying states has first been identified in studies of cold plasmas [9]. The electrons trapped in the space-charge cloud make many oscillations through the cloud before the trapping potential diminishes due to the expansion of the ion/electron cloud. While the electrons oscillate through the space-charge potential, they frequently collide with the Rydberg atoms that are embedded within the space charge cloud.

While the space-charge cloud expands, it releases the trapped electrons, which reach our MCP detector. The duration of the resultant current directly reveals the lifetime of the electron trap. Fig. 2 demonstrates that our electron trap lives for about 25 μs. The lifetime increases with decreasing voltage applied to the MCP. This observation is consistent with the reasonable assumption that the weak electric field at the location of the atom trap is dominated by the MCP stray field. A larger MCP field increases the electric field at the location of the atom cloud, thereby accelerating the disintegration of the space-charge electron trap. These findings are in agreement with previous work [9]. We estimate that under our conditions of order 2000 electrons need to leave the atom cloud to retain most of the subsequently produced electrons.

Due to the presence of the electron trap, the interaction time to be inserted into Eq. (1) is ~ 50 μs. If there was no electron trapping mechanism, the thermal electrons would escape the Rydberg atom cloud within of order 10 ns. Thus, the electron-trapping mechanism enhances the probability of l-mixing collisions by a factor > 1000. The enhancement of the interaction time due to an electron trapping mechanism is critical in our explanation of the l-mixing, as it strongly reduces the values of the collision cross section and the electron density required in order to satisfy Eq. (1).

4.5 L-mixing of Low-Angular-Momentum States of Rb

So far, we found that under conditions of Fig. 1 a few thousand electrons with energies of order 10 meV will be accumulated in a volume of about 1 mm^3 for a time of order 50 μs. The estimated electron density thus is 10^6 cm^{-3} $< n_e <$ 10^7 cm^{-3}. To finally establish the validity of Eq. (1), the l-mixing collision cross sections of ns and nd Rydberg states of rubidium need to be considered.

The mechanism of l-changing collisions of low-angular-momentum Rydberg states of alkali atoms is illustrated in Fig. 6, where we consider the Stark map of a rubidium Rydberg atom in the vicinity of $21d$. In rubidium, states with $l > 3$ are essentially hydrogenic, i.e. their energies at zero electric field are $-1/2n^2$. As an electric field is applied, the hydrogenic states display linear Stark effect, i.e. they fan out in a linear manner. Infinitesimally small static or dynamic electric fields will be sufficient to cause mixing and "Stark beats" between the hydrogenic states [13]. The situation is different if the initial state is a low-angular momentum state with a significant quantum defect. In that case, the critical electric field required to achieve efficient l-mixing is the field at which the initial state and the next-

nearest hydrogenic manifold begin to overlap. For instance, as seen in Fig. 6, the state 21d would exhibit significant l-mixing only for fields larger than 8×10^{-8} at.un. $= 4$ V/cm. Therefore, the l-mixing of an initially low-l Rydberg atom requires a much closer collision with a charged particle than the l-mixing of hydrogenic atoms. This close collision acts as a "bottleneck" process.

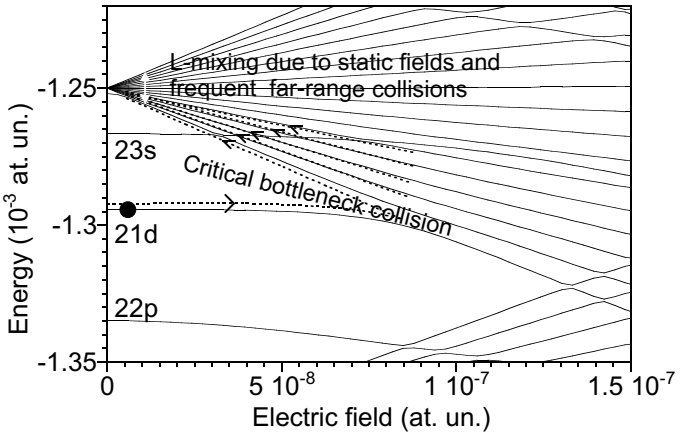

Figure 6. Stark map of Rb near n=20 illustrating l-mixing collisions of low-l Rydberg atoms. A first close "bottleneck" collision promotes the atom from its state with large quantum defect into a hydrogenic state with essentially zero quantum defect. After the bottleneck collision, far-range collisions and static fields lead to further l-mixing within the hydrogenic manifold.

In Fig. 6, in the critical bottleneck collision an electron approaches a $21d$ Rydberg atom close enough that its electric field at the location of the Rydberg atom exceeds 8×10^{-8} at.un., i.e. the field above which the levels of the hydrogenic manifold of n=20 mix with the $21d$ level. As the electron moves away and the electric field decreases again, there exists a large probability that the atom remains in the hydrogenic manifold. We find in calculations that generally the bottleneck collisions that transfer atoms from their initial s or d-states into hydrogenic states profoundly increase the angular momentum; typically, after the bottleneck collisions the expectation value of l is $\approx n/2$. After a bottleneck collision, weak static stray electric fields and far-range collisions are likely to further randomize the population distribution within the hydrogenic manifold [13].

4.6 L-mixing Cross Sections of Rb s and d-States

For a quantitative estimate of whether Eq. (1) is satisfied, we have numerically solved the time-dependent Schrödinger equation for collisions between Rydberg atoms and singly charged particles. We have used the"impact approximation", in which the charged particle that collides with the Rydberg atom is treated classically and moves on a straight trajectory with constant velocity and impact parameter b. During the collision, the electric field created by the charged particle at the location of the Rydberg atom gradually reverses its direction. The field is assumed to be homogeneous, *i.e.* only electric-dipole couplings between Rydberg states are considered. For given initial state $|n_0, l_0, m_0\rangle$ and

impact parameter b, the calculation yields a final state $\sum_{n,l,m} c_{n,l,m}|n,l,m\rangle$. Based on the qualitative discussion in Sec. 4.5, we consider a collision to be a successful l-mixing collision if it promotes the atom from its initial low-l state ($l < 3$ for Rb) into a state $l > 3$. In order to be certain that we do not overestimate the l-mixing cross sections, we do not consider collision-induced transitions into f-states ($l = 3$) as successful l-mixing.

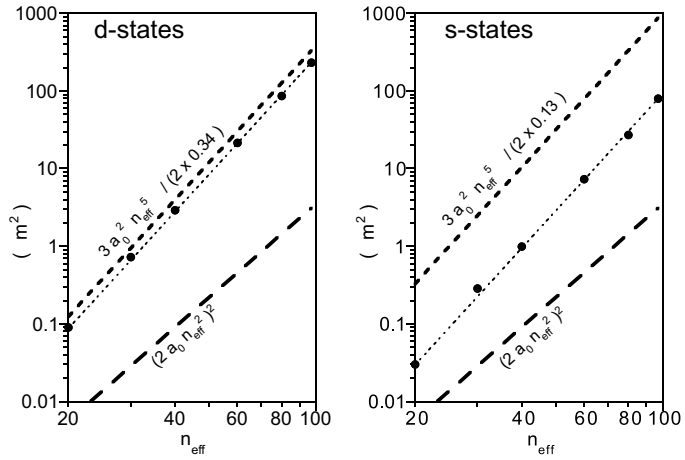

Figure 7. l-mixing cross sections for an electron energy of 5 meV for d (left) and s (right) states of rubidium vs. the effective quantum number. The cross sections (filled circles) are well fitted by functions $\propto n_{\rm eff}^5$ (dotted). The d-cross sections are close to the value $b_c^2\pi$ (short-dashed), where b_c is the critical distance explained in the text. The s-cross sections are much smaller than the value $b_c^2\pi$. All l-mixing cross sections are much larger than the estimated ionization cross sections for collisions between Rydberg atoms and electrons (long-dashed).

For a given impact parameter b, the l-mixing probability is $P_{l>3}(b) = \sum_{n,l>3,m} |c_{n,l,m}|^2$, and the average angular momentum is $\langle l\rangle = \sum_{n,l,m} l|c_{n,l,m}|^2$. Averaging over the impact parameter yields for the collision cross section

$$\sigma = \int_{b_{\rm min}}^{b_{\rm max}} P_{l>3}(b) 2\pi b db \tag{2}$$

The lower cutoff $b_{\rm min}$ is not very important due to the factor b in the integrand, and may be taken to be equal to the size of the Rydberg atom. For smaller collision parameters, the ionization of the Rydberg atom will be the dominant outcome of the collision. Typically, $P_{l>3}(b)$ is found to be significant for $b \le b_c$, where b_c is a critical distance $b_c = \sqrt{3n^5/2\tilde{\delta}}$ at.un. and $\tilde{\delta}$ is the non-integer part of the quantum defect. Beyond $b = b_c$, $P_{l>3}(b)$ tends to rapidly go to zero. The upper cutoff $b_{\rm max}$ in Eq. (2) is chosen by requiring $P_{l>3}(b)$ to drop below $\sim 1\%$. This condition typically occurs at $b \sim 1.5 b_c$. Since we assume isotropic conditions, for states other than s-states we average the results of Eq. (2) over the m-quantum number of the initial state.

In Fig. 7, the l-mixing collision cross sections for s and d-states are shown vs. the effective quantum number for a fixed electron energy of 5 meV. For s-states, the cross

sections are about a factor of three smaller than for the nearby d-states, but still follow an $n_{\rm eff}^5$-dependence. In all cases, the l-mixing cross sections are much larger than the estimated cross sections of ionizing collisions. The typical dependence of the cross sections on the electron energy is shown in Fig. 8.

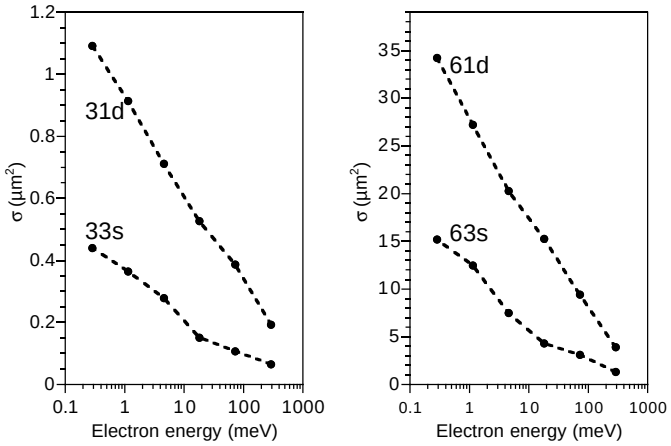

Figure 8. l-mixing collision cross section vs. kinetic energy of an electron colliding with a Rb Rydberg atom in the indicated initial states.

Using the calculated cross sections, $t_{\rm int} = 50$ μs, $v = 50000$ m/s, and the range of the electron density mentioned at the beginning of Sec. 4.5, we find that Eq. (1) holds for the conditions of Fig. 1. We note that without the electron trap discussed in Sec. 4.4 we would have to use $t_{\rm int} \sim 10$ ns in Eq. (1), and that equation would be invalidated by a couple of orders of magnitude.

5 Other Considerations

The critical role of the electron trap is made further evident by the near-absence of the s-peaks in Fig. 1. We have estimated that, if the Rydberg transitions are not saturated, the yield of early electrons from the s-states is only $\sim$1/10 that of the d-states [10]. We therefore believe that the s-states are often missing in delayed electron spectra such as Fig. 1 because the number of early electrons created on the s-lines may not be sufficient to produce a filled electron trap. We have performed some experiments [10] that support this hypothesis.

A possible mechanism for transforming low-l into high-l Rydberg states is rapid ionization of the initial Rydberg atoms followed by recombination into high-l states [7]. If such recombination were significant in our studies, the electron signal for $\lambda < \lambda_{\rm ion}$, where a plasma is directly created, would be comparable to the average signal level right below the ionization threshold, $\lambda > \lambda_{\rm ion}$. This is not the case, as seen in Fig. 1. We believe that in our system the plasma densities are not high enough to observe significant recombination into high-l Rydberg states.

Using a system similar to ours, recent investigations have shown that when an electron trap forms, Rydberg atom-electron ionizing collisions may lead to nearly complete ionization

of the Rydberg cloud [1]. We have also observed indications of such large-scale ionization. We have noted in Sec. 3.3 that the peaks underneath the dashed line in Fig. 4, where the Rydberg atom density is a few 10^9 cm^{-3}, do not have a counterpart in the corresponding delayed electron signal. This finding suggests that in Fig. 4 collisional ionization of Rydberg atoms dominates the trap loss in the range $n > 40$. To explain the observed behavior, we note that the cross sections of ionizing Rydberg atom-electron collisions are smaller than the ones for l-mixing only by a factor of order n [11]. Thus, ionization should override the effect of l-mixing if the quantity P in Eq. (1) reaches a value of order n. In Fig. 4, this appears to be the case for $n > 40$. Full-scale ionization removes atoms from the atom trap with an efficiency larger than that of l-mixing and subsequent thermal ionization. This fact may explain the relatively large values of X underneath the dashed line in Fig. 4.

6 Conclusion

We have found that cold Rydberg gases in a room-temperature thermal radiation field can exhibit production of high-l Rydberg states and subsequent slow thermal ionization. The effect hinges on the temporary existence of a space-charge electron trap. The observed dynamics may be used as a simple method to generate a statistical mixture of high-l Rydberg atoms. We plan to use such samples of atoms in efforts to trap cold Rydberg atoms.

Acknowledgments

We acknowledge support by the NSF (Grant PHY-9875553) and by the Chemical Sciences, Geosciences and Biosciences Division of the Office of Basic Energy Sciences, Office of Science, U. S. Department of Energy. We thank Prof. P. H. Bucksbaum for inspiring discussions and generous loaning of equipment.

References

1. M.P. Robinson *et al*, *Phys. Rev. Lett.* **85**, 4466 (2000).
2. G. Vitrant *et al*, *J. Phys.* **B 15**, L49 (1982).
3. W. R. Anderson, J. R. Veale, T. F. Gallagher, *Phys. Rev. Lett.* **80**, 249 (1998).
4. I. Mourachko *et al Phys. Rev. Lett.* **80**, 253 (1998).
5. D. Jaksch *et al*, *Phys. Rev. Lett.* **85**, 2208 (2000).
6. C. H. Greene, *Phys. Rev. Lett.* **85**, 2458 (2000).
7. T. C. Killian *et al*, *Phys. Rev. Lett.* **86**, 3759 (2001).
8. E. W. Schlag, R. D. Levine, *Comm. At. Mol. Phys.* **33**, 159 (1997), W. A. Chupka, *J. Chem. Phys.* **99**, 4580 (1993), P. Bellomo, D. Farelly, T. Uzer, *J. Chem. Phys.* **108**, 5259 (1998).
9. T. C. Killian *et al*, *Phys. Rev. Lett.* **83**, 4776 (1999).
10. S. K. Dutta *et al* , *Phys. Rev. Lett.* **86**, 3993 (2001).
11. T. F. Gallagher, *Rydberg Atoms*, Cambridge University Press, Cambridge 1994.
12. X. Sun, K. B. MacAdam, *Phys. Rev.* **A 47**, 3913 (1993).
13. D. L. Dorofeev, B. A. Zon, *J. Chem. Phys.* **106**, 9609 (1997), D. Vrinceanu, M. R. Flannery, *Phys. Rev. Lett.* **85**, 4880 (2000), D. Vrinceanu, M. R. Flannery, *Phys. Rev.* **A 63**, 032701 (2001).